

1

Supporting Information

2

for

3

Single-Molecule Determinations of the Phase- and Facet-

4

Dependent Adsorption of Alginate on Iron Oxide

5

6

Hang Zhai and Lijun Wang*

7

College of Resources and Environment, Huazhong Agricultural University, Wuhan 430070,

8

China

9

10

11 SI Tables (1-2)

12 SI Figures (1-8)

13 SI References (1-3)

14

15

16

17

18

19

20 **Table S1.** Values of f_{eq} and ΔG_B extracted from fitting the Friddle-Noy-DeYoreo model
 21 to the DFS data. Values are present as mean \pm standard deviation ($n = 3$).

pH	<i>IS</i> (mM)	Electrolyte	Phase/Face	f_{eq} (pN)	ΔG_B (kJ/mol)
5.0	10	NaCl	Fe_xO_y	276.56 ± 11.75	112.38 ± 4.78
5.0	10	NaCl	(10 $\bar{1}$ 0)	248.72 ± 18.33	101.07 ± 7.45
5.0	10	NaCl	(11 $\bar{2}$ 0)	216.17 ± 11.44	87.84 ± 4.65
5.0	10	NaCl	(0001)	171.32 ± 9.53	69.62 ± 3.87
7.0	10	NaCl	Fe_xO_y	256.41 ± 7.28	104.19 ± 2.96
7.0	10	NaCl	(10 $\bar{1}$ 0)	204.84 ± 7.86	83.24 ± 3.20
7.0	10	NaCl	(11 $\bar{2}$ 0)	173.28 ± 17.81	70.41 ± 7.23
7.0	10	NaCl	(0001)	145.96 ± 13.71	59.31 ± 5.57
9.0	10	NaCl	Fe_xO_y	202.56 ± 9.64	82.31 ± 3.92
9.0	10	NaCl	(10 $\bar{1}$ 0)	158.96 ± 10.22	64.59 ± 4.15
9.0	10	NaCl	(11 $\bar{2}$ 0)	164.43 ± 10.51	66.82 ± 4.27
9.0	10	NaCl	(0001)	142.58 ± 8.95	57.94 ± 3.63
7.0	1000	NaCl	Fe_xO_y	182.31 ± 5.70	74.08 ± 2.31
7.0	1000	NaCl	(10 $\bar{1}$ 0)	143.79 ± 11.19	58.43 ± 4.55
7.0	1000	NaCl	(11 $\bar{2}$ 0)	153.44 ± 12.43	62.35 ± 5.05
7.0	1000	NaCl	(0001)	142.02 ± 13.46	57.71 ± 5.47
7.0	100	NaCl	Fe_xO_y	204.74 ± 19.63	83.20 ± 7.98
7.0	100	NaCl	(10 $\bar{1}$ 0)	163.01 ± 3.99	66.24 ± 1.62
7.0	100	NaCl	(11 $\bar{2}$ 0)	173.28 ± 17.80	72.54 ± 4.41
7.0	100	NaCl	(0001)	145.96 ± 13.71	61.26 ± 3.44
7.0	1	NaCl	Fe_xO_y	267.32 ± 9.10	108.63 ± 3.70
7.0	1	NaCl	(10 $\bar{1}$ 0)	210.98 ± 11.21	85.74 ± 4.56
7.0	1	NaCl	(11 $\bar{2}$ 0)	209.41 ± 12.77	85.09 ± 5.19
7.0	1	NaCl	(0001)	167.95 ± 5.93	68.25 ± 2.41
7.0	10	CaCl ₂	(10 $\bar{1}$ 0)	224.07 ± 9.94	91.05 ± 4.04
7.0	10	CdCl ₂	(10 $\bar{1}$ 0)	251.53 ± 10.01	102.21 ± 4.16
7.0	10	Na ₂ HAsO ₄	(10 $\bar{1}$ 0)	137.18 ± 12.09	55.74 ± 5.01

22

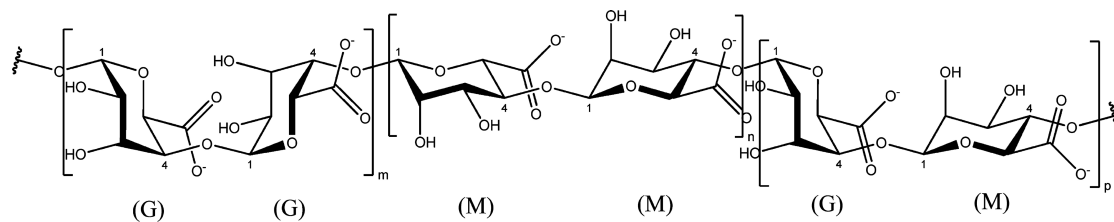
23

24 **Table S2.** Chemical formulae and its corresponding Raman bands for hematite and
 25 amorphous Fe_xO_y . The wavenumbers of the most prominent bands in Raman signals of
 26 individual minerals are in bold.

Minerals	Distinguishing Raman shift (cm^{-1})	Reference
Hematite	222, 230, 290 , 408, 490, 607	1
Amorphous Fe_xO_y	361, 508, 707 , 1045	2

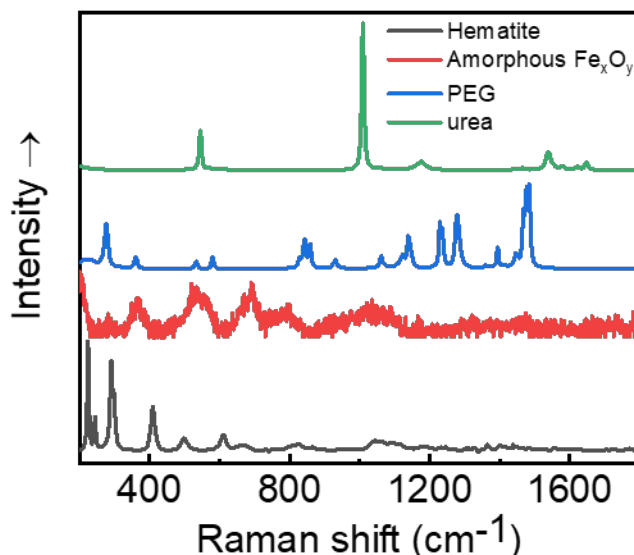
27

28



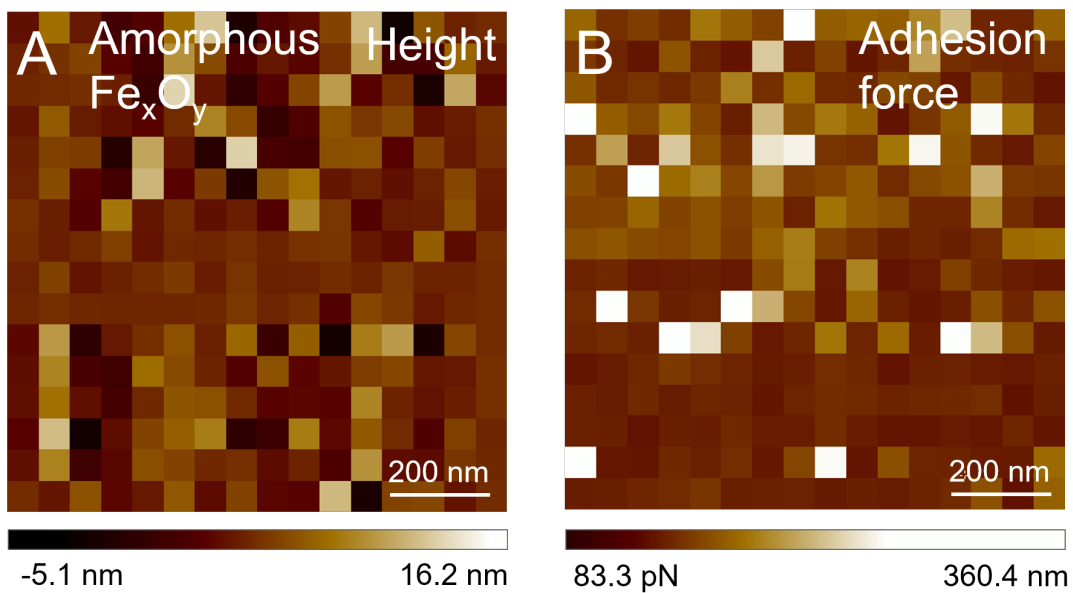
29 **Figure S1.** The structure of alginate showing that alginate is a linear polysaccharide of
 30 (1→4) linked α -L-guluronate(G) and β -D-mannuronate (M).³ Copyright 2011
 31 American Chemical Society.

32



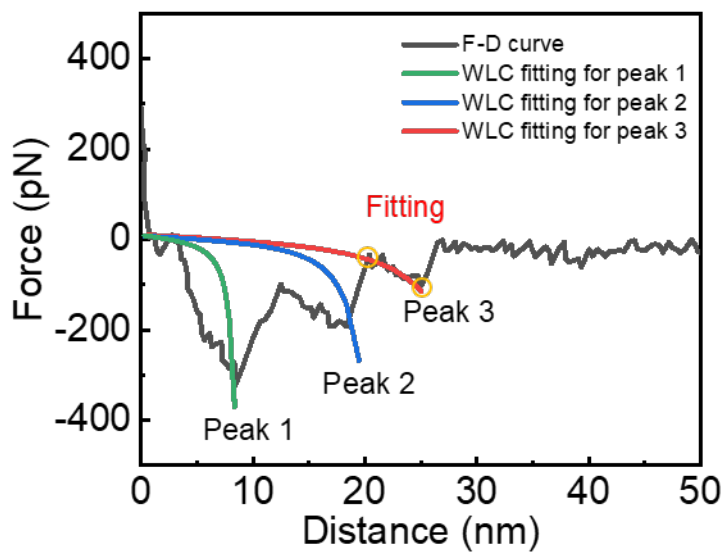
33 **Figure S2.** Raman spectra collected from hematite (black), amorphous Fe_xO_y (red),
 34 polyethylene glycol (PEG, blue), and urea (green), showing that no PEG and urea

35 residues were present.



36

37 **Figure S3.** (A) The height and (B) the corresponding adhesion force of amorphous
38 Fe_xO_y measured with alginate-decorated tip in the force-volume mode showing the
39 adhesion force is independent of the height.

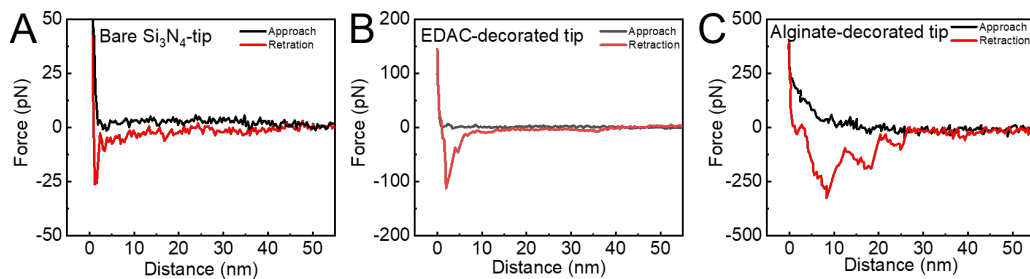


40

41 **Figure S4.** A representative force-distance curve showing only the last rupture event
42 (Peak 3) fitted into the WLC model.

43

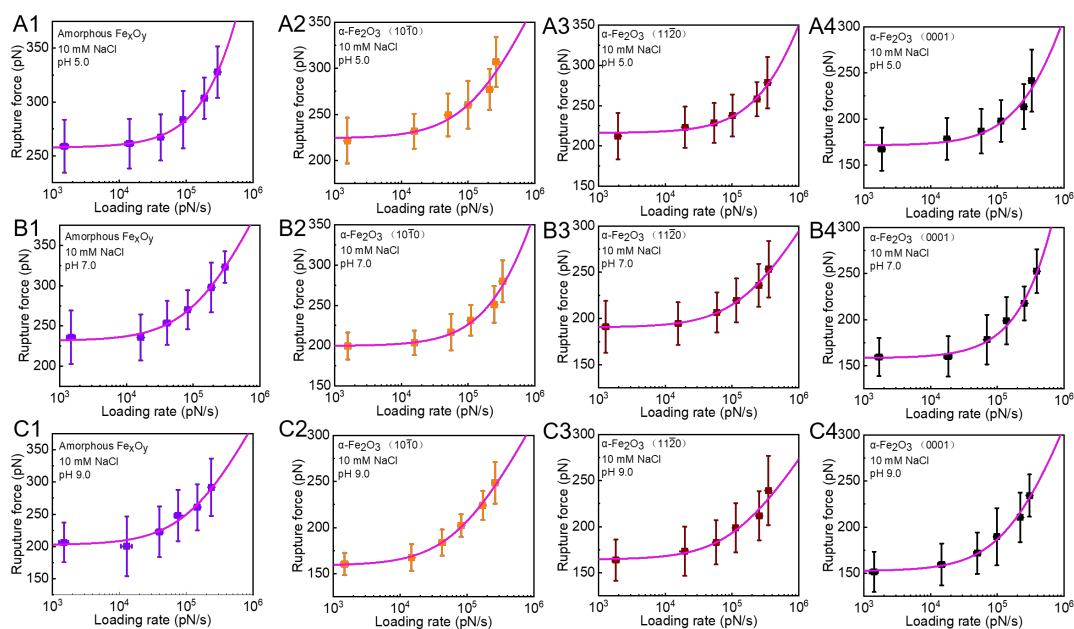
44



48

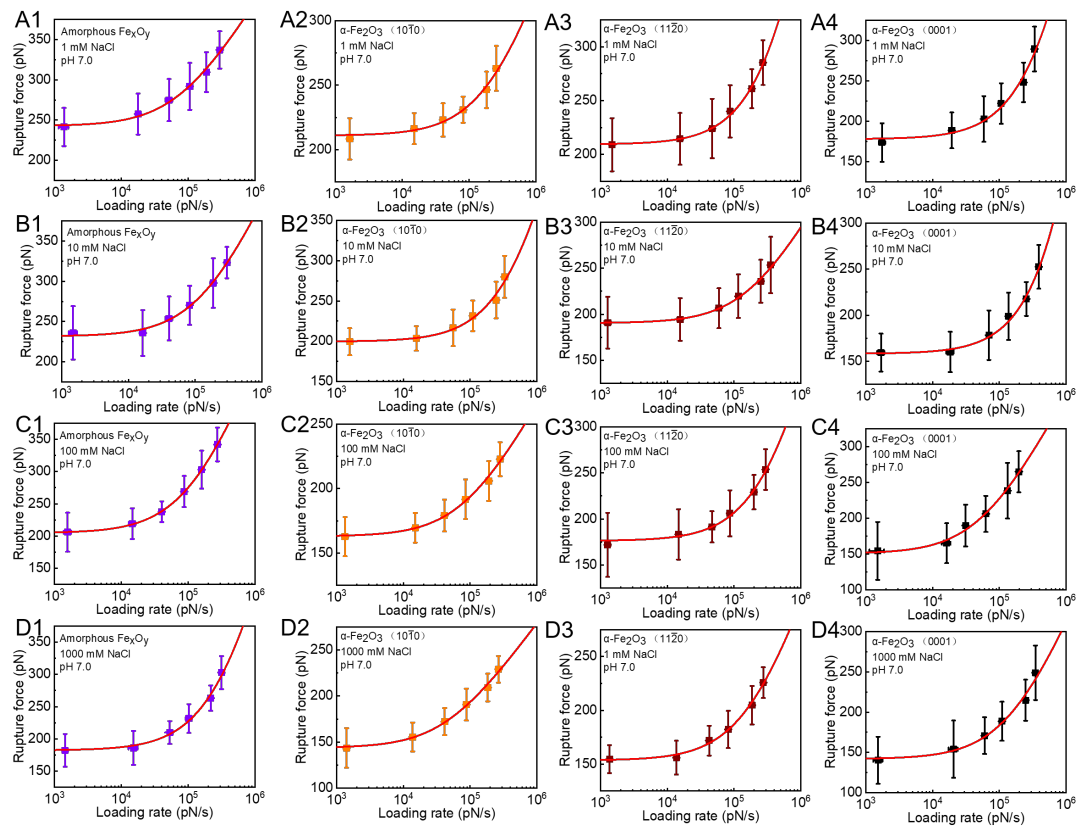
45 **Figure S5.** Representative force curves obtained with the (A) bare Si_3N_4 tip, (B) linker
46 (1-(3-dimethylaminopropyl)-3-ethylcarbodiimide hydrochloride, EDAC)-coating tip
47 and (C) alginate-decorated tip on the hematite ($10\bar{1}0$) surface.

49



50 **Figure S6.** Dynamic force spectra (DFS) of alginate binding to amorphous Fe_xO_y or
51 hematite ($\alpha\text{-Fe}_2\text{O}_3$) with the ($10\bar{1}0$), ($11\bar{2}0$), and (0001) faces in 10 mM NaCl solutions
52 at (A1-A4) pH 5.0, (B1-B4) pH 7.0 and (C1-C4) pH 9.0.

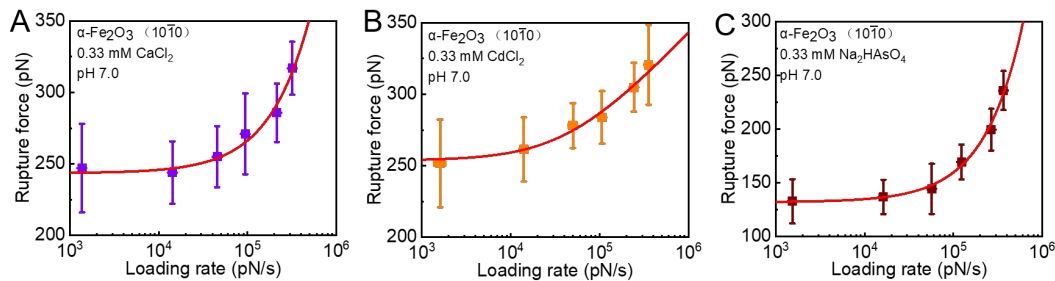
53



54 **Figure S7.** Dynamic force spectra (DFS) of alginate binding to amorphous Fe_xO_y or
55 hematite ($\alpha\text{-Fe}_2\text{O}_3$) with the (10̄0), (11̄20), and (0001) faces in solutions at (A1-A4) 1,
56 (B1-B4) 10, (C1-C4) 100, and (D1-D4) 1000 mM at pH 7.0.

57

58



59 **Figure S8.** Dynamic force spectra (DFS) of alginate binding to the (10̄0) face of
60 hematite ($\alpha\text{-Fe}_2\text{O}_3$) in solutions (total IS = 10 mM and pH 7.0) containing (A) 0.33 mM
61 CaCl_2 , (B) 0.33 mM CdCl_2 , or (C) 0.33 mM Na_2HAsO_4 .

62 **SI References.**

- 63 1. M. A. Legodi, D. de Waal, The preparation of magnetite, goethite, hematite and
64 maghemite of pigment quality from mill scale iron waste. *Dyes Pigments*, 2007,
65 **74**, 161–168.
- 66 2. S. Das, and M. J. Hendry, Application of Raman spectroscopy to identify iron
67 minerals commonly found in mine wastes. *Chem. Geol.*, 2011, **290**, 101-108.
- 68 3. P. Agulhon, M. Robitzer, L. David, and F. Quignard, Structural regime
69 identification in ionotropic alginate gels: influence of the cation nature and
70 alginate structure. *Biomacromolecules*, 2011, **13**, 215-220.

71